


## Article

# Variable Structure Disturbance Observer Based Dynamic Surface Control of Electrohydraulic Systems with Parametric Uncertainty

Shuai Li, Ke Zhu, Liang Chen, Yao Yan and Qing Guo \* 

School of Aeronautics and Astronautics, University of Electronic Science and Technology of China, Chengdu 611731, China; shuaili66@126.com (S.L.); zk\_814575043@163.com (K.Z.); hn576504256@163.com (L.C.); y.yan@uestc.edu.cn (Y.Y.)

\* Correspondence: guoqinguestc@uestc.edu.cn

**Abstract:** This paper focuses on the position tracking control issue of electrohydraulic systems (EHS). The dynamical model of EHS is introduced in the first place, based on which a type of Variable Structure Disturbance Observer (VSDO) is constructed for EHS to estimate the parametric uncertainty the EHS possesses. Then, a backstepping controller is designed under VSDO to realize the high precision position tracking purpose. To avoid the phenomenon of differential explosion, a dynamic surface control method is adopted in this paper, which improved the position tracking control performance of EHS. The proposed theoretical results are verified by numerical simulation and experiment to illustrate the feasibility.

**Keywords:** variable structure disturbance observers; electrohydraulic systems; dynamic surface control; backstepping iteration; parametric uncertainty



**Citation:** Li, S.; Zhu, K.; Chen, L.; Yan, Y.; Guo, Q. Variable Structure Disturbance Observer Based Dynamic Surface Control of Electrohydraulic Systems with Parametric Uncertainty. *Energies* **2022**, *15*, 1671. <https://doi.org/10.3390/en15051671>

Academic Editors: Hu Shi and Oscar Barambones

Received: 30 January 2022

Accepted: 20 February 2022

Published: 23 February 2022

**Publisher's Note:** MDPI stays neutral with regard to jurisdictional claims in published maps and institutional affiliations.



**Copyright:** © 2022 by the authors. Licensee MDPI, Basel, Switzerland. This article is an open access article distributed under the terms and conditions of the Creative Commons Attribution (CC BY) license (<https://creativecommons.org/licenses/by/4.0/>).

## 1. Introduction

As a kind of conventional electromechanical system, electrohydraulic systems (EHS) are widely used in engineering practices, such as marine engineering, power generation projects, automobile engineering, safety engineering and so on [1–6] due to the fact that EHS possesses the characteristics of high energy density and accurate control ability. Actually, a series of research achievements on the control issue of EHS has been published in recent years with plentiful advanced control methods proposed, such as backstepping control [7,8], sliding mode control [9,10], robust integral control [11,12], neural network control [13,14], and feedback linearization control [15,16]. A sliding mode control possesses a simple structure as a controller, but it is difficult to avoid the tremor in the process of control. A robust integral controller has a good performance in the steady state process but is poor in transient performance. A neural network controller can achieve the control purpose quickly but may become trapped in a locally optimal solution and, thus, obtain a poor control result. The feedback linearization control method is not well studied in EHS; only the proportion adjustment is considered at present, and the control effect is still not ideal. Due to the foregoing, the most commonly used controller in research of EHS is a backstepping controller. Although its controller design steps are a bit cumbersome, the control performance on EHS is highly desirable.

As is known, an EHS can be modeled as a three-order nonlinear differential equation. During the backstepping controller design procedure, two virtual control parameters should be defined for the first and second order of the EHS model. By an iterative process, the control input can be designed. During the iterative process, two virtual control parameters will be differentiated more than once, and, thus, a differential explosion may occur. In order to avoid the effect of the differential explosion on the control performance of EHS, a control strategy, called dynamic surface control, based on backstepping is

introduced [17–20]. By constructing a dynamic surface for the virtual control variables, the differential explosion will be averted.

On the other hand, since the parametric uncertainty is a common presence in electromechanical systems, how to handle this kind of uncertainty is also a critical issue. In the past decades, some kinds of disturbance observers have been introduced to EHS to compensate for the position tracking error caused by parametric uncertainty, such as an adaptive observer, a high gain observer, an extended state observer, and so on. All of these observers possess the ability to accurately estimate the parametric uncertainty and, thus, enhance the position tracking control performance of EHS. As the structural design of the observer becomes more and more complex, the estimation performance of the observer is improving. In recent years, a novel kind of observer, which is designed via a variable structure method has been proposed for dynamical systems, and this variable structure disturbance observer (VSDO) possesses a faster estimation ability for the uncertainties of dynamical systems [21–24].

In this paper, we propose a novel position tracking control strategy for EHS. First, a group of variable structure disturbance observers are designed to estimate the parametric uncertainty of EHS. Then, different from the conventional backstepping strategy, a dynamic surface control method based on the proposed VSDO is presented to realize the position tracking control purpose of the EHS. The effectiveness of the proposed theoretical conclusion is verified by simulation and experiment.

The rest of the paper is organized as follows: The modeling and problem formulation for EHS is presented in Section 2. The VSDO design processes are provided in Section 3. The controller design and stability analysis processes are provided in Section 4. The simulation results are shown in Section 5, and the experimental results are provided in Section 6. Finally, Sections 7 and 8 discuss and conclude this paper.

## 2. Preliminaries

As Figure 1 exhibits, one EHS consists of a motor, a pump, a relief valve, a servo valve, and a cylinder. The motor drives the pump, and then the pump supplies the pressure  $p_s$  to the relief valve. The load pressure  $p_L$  has a direct relation with the motion of the cylinder. We define the vector  $[x_1, x_2, x_3]^T = [y, \dot{y}, A_p p_L]^T$ ; then, the considered EHS can be described as

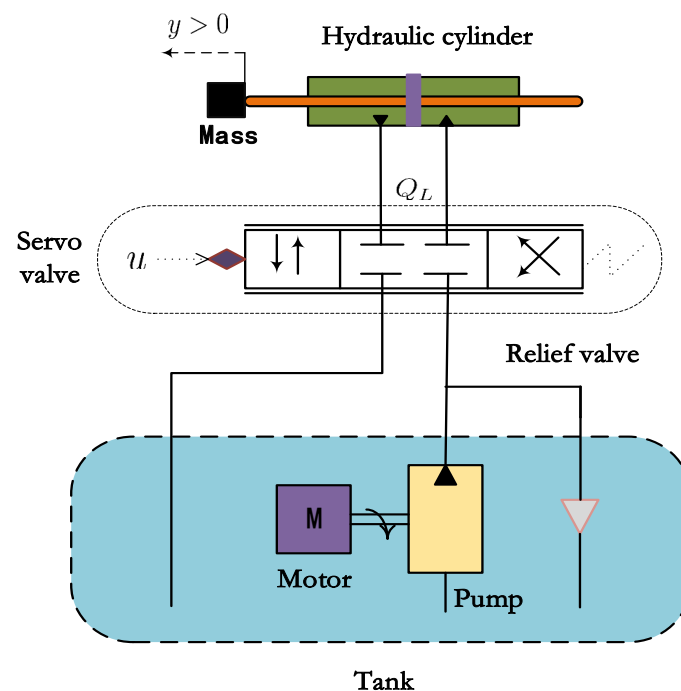


Figure 1. The EHS composition.

$$\begin{cases} \dot{x}_1 = x_2 \\ \dot{x}_2 = \frac{1}{m}(x_3 - Kx_1 - bx_2) \\ \dot{x}_3 = -\frac{4\beta_e A_p^2}{V_t}x_2 - \frac{4\beta_e C_{tl}}{V_t}x_3 + \frac{4\beta_e C_d \bar{w} K_{sv} A_p}{V_t \sqrt{\rho}} \sqrt{p_s - \text{sgn}(u)x_3/A_p} u \\ y = x_1 \end{cases} \quad (1)$$

where  $\text{sgn}(\cdot)$  is given by

$$\text{sgn}(u) = \begin{cases} 1, & u > 0 \\ 0, & u = 0, \\ -1, & u < 0 \end{cases}$$

and other parameters are introduced in the nomenclature section.

**Assumption 1.** For the EHS considered in this paper, the supply pressure of EHS is a constant value, and the runoff pressure of EHS is zero. The external load disturbance is neglected.

**Remark 1.** The parameters  $C_d$ ,  $\rho$ ,  $K$ ,  $b$ ,  $\beta_e$ , and  $C_{tl}$  of EHS are all uncertain positive constants.

Based on Remark 1, the uncertain EHS can be described as:

$$\begin{cases} \dot{x}_1 = x_2 \\ \dot{x}_2 = \bar{f}_2(x_1, x_2) + \bar{g}_2 x_3 + \Delta_2(x_1, x_2) \\ \dot{x}_3 = \bar{f}_3(x_2, x_3) + \bar{g}_3(x_3, u)u + \Delta_3(x_1, x_2, x_3) \\ y = x_1 \end{cases} \quad (2)$$

where

$$\begin{aligned} \bar{f}_2(x_1, x_2) &= -(\bar{K}x_1 + \bar{b}x_2)/m \\ \bar{g}_2 &= 1/m \\ \bar{f}_3(x_2, x_3) &= -\frac{4\bar{\beta}_e A_p^2}{V_t}x_2 - \frac{4\bar{\beta}_e \bar{C}_{tl}}{V_t}x_3 \\ \bar{g}_3(x_3, u) &= \frac{4\bar{\beta}_e \bar{C}_d \bar{w} K_{sv} A_p}{V_t \sqrt{\rho}} \sqrt{p_s - \text{sgn}(u)x_3/A_p} \end{aligned}$$

are nominal terms, and

$$\begin{aligned} \Delta_2(x_1, x_2) &= -(\Delta Kx_1 + \Delta bx_2)/m \\ \Delta_3(x_1, x_2, x_3) &= \Delta f_3(x_2, x_3) + \Delta g_3(x_1, x_2, x_3) \end{aligned}$$

are uncertain items.

**Assumption 2.** For two uncertain items  $\Delta_2$  and  $\Delta_3$ , the following inequality is satisfied

$$|\Delta_i| \leq D_i, \quad i \in \{2, 3\}$$

where  $D_i$  are known positive constants.

### 3. Variable Structure Disturbance Observer Design

This section will design two disturbance observers to estimate the uncertain items  $\Delta_2$  and  $\Delta_3$  of EHS. Firstly, we define two auxiliary variables as:

$$\begin{cases} s_2 = v_2 - x_1 \\ s_3 = v_3 - x_2 \end{cases} \quad (3)$$

where  $v_2$  and  $v_3$  are constructed as

$$\begin{cases} \dot{v}_2 = -k_{d2}s_2 - D_2\text{sgn}(s_2) + f_2 + g_2x_3 \\ \dot{v}_3 = -k_{d3}s_3 - D_3\text{sgn}(s_3) + f_3 + g_3u \end{cases} \quad (4)$$

where  $k_{di}$  and  $D_i$  are all positive for  $i \in \{2, 3\}$ . Then, the estimated values of VSDO for the parametric uncertainty of EHS are given by

$$\hat{\Delta}_i = -k_{di}s_i - D_i\text{sgn}(s_i), \quad i \in \{2, 3\} \quad (5)$$

**Theorem 1.** *Considering the system (2) together with the VSDO designed in (3)–(5), the disturbance estimation errors of  $\tilde{\Delta}_2$  and  $\tilde{\Delta}_3$  will converge to an equilibrium point.*

**Proof.** For the uncertain item  $\Delta_2$ , a Lyapunov function is constructed as

$$V_{s_2} = s_2^2/2$$

and, thus, the derivative of  $V_2$  is given by

$$\begin{aligned} \dot{V}_{s_2} &= s_2\dot{s}_2 \\ &= s_2(\dot{v}_2 - \dot{x}_2) \\ &= s_2(-k_{d2}s_2 - D_2\text{sgn}(s_2) - \Delta_2) \\ &\leq -k_{d2}s_2^2 - D_2s_2\text{sgn}(s_2) + |s_2||\Delta_2|. \end{aligned} \quad (6)$$

Based on Assumption 2, the inequality (6) can be rewritten as

$$\dot{V}_{s_2} \leq -k_{d2}s_2^2 - D_2|s_2| + |s_2||\Delta_2| \leq -k_{d2}s_2^2 \leq 0,$$

and the estimation error is

$$\begin{aligned} \tilde{\Delta}_2 &= \hat{\Delta}_2 - \Delta_2 \\ &= -k_{d2}s_2 - D_2\text{sgn}(s_2) + f_2 + g_2x_3 - \dot{x}_2 \\ &= \dot{v}_2 - \dot{x}_1 \\ &= \dot{s}_2. \end{aligned} \quad (7)$$

Then, for the uncertain item  $\Delta_3$ , a Lyapunov function is constructed as

$$V_{s_3} = s_3^2/2$$

and thus the derivative of  $V_2$  is given by

$$\begin{aligned} \dot{V}_{s_3} &= s_3\dot{s}_3 \\ &= s_3(\dot{v}_3 - \dot{x}_3) \\ &= s_3(-k_{d3}s_3 - D_3\text{sgn}(s_3) - \Delta_3) \\ &\leq -k_{d3}s_3^2 - D_3s_3\text{sgn}(s_3) + |s_3||\Delta_3| \end{aligned} \quad (8)$$



Based on Assumption 2, the inequality (6) can be rewritten as

$$\dot{V}_{s_3} \leq -k_{d3}s_3^2 - D_3|s_3| + |s_3||\Delta_3| \leq -k_{d3}s_3^2 \leq 0$$

and the approximation error as

$$\begin{aligned} \tilde{\Delta}_3 &= \hat{\Delta}_3 - \Delta_3 \\ &= -k_{d3}s_3 - D_3\text{sgn}(s_3) + f_3 + g_3u - \dot{x}_3 \\ &= \dot{v}_3 - \dot{x}_2 \\ &= \dot{s}_3 \end{aligned} \quad (9)$$

The inequality (6) and (8) yields that the auxiliary variables  $s_2$  and  $s_3$  will converge to the equilibrium point, which also demonstrates that the estimation errors  $\tilde{\Delta}_2$  and  $\tilde{\Delta}_3$  will converge to the equilibrium point. This concludes the proof.  $\square$

#### 4. Dynamic Surface Controller Design

In this section, a backstepping control based position tracking control strategy via dynamic surface is proposed. As the first step, we define a group of error functions as:

$$\begin{cases} z_1 = y - y_d \\ z_2 = x_2 - \alpha_1 + s_2 \\ z_3 = x_3 - \alpha_2 + s_3 \end{cases} \quad (10)$$

where  $y_d$  is the expected displacement, and  $\alpha_i, i \in \{1, 2\}$  are the virtual control variables in backstepping controller. Based on (2), the time derivation of (10) can be obtained as

$$\begin{cases} \dot{z}_1 = x_2 - \dot{y}_d \\ \dot{z}_2 = \bar{f}_2(x_1, x_2) + \bar{g}_2x_3 + \Delta_2(x_1, x_2) - \dot{\alpha}_1 + \dot{s}_2 \\ \dot{z}_3 = \bar{f}_3(x_2, x_3) + \bar{g}_3(x_3, u)u + \Delta_3(x_1, x_2, x_3) - \dot{\alpha}_2 + \dot{s}_3. \end{cases} \quad (11)$$

The specific control strategy is provided in the following. To overcome the differential explosion during the iteration in backstepping control, two dynamic surfaces are given by a first-order filter form as:

$$\tau_i \dot{\alpha}_i + \alpha_i = \beta_i, \quad \alpha_i(0) = \beta_i(0), \quad i \in \{1, 2\} \quad (12)$$

where  $\beta_i$  are stabilizing filter functions and  $\tau_i$  are the coefficients of the dynamic surfaces. We define  $S_i = \alpha_i - \beta_i$  for  $i \in \{1, 2\}$ ; then, we can obtain from (12) that  $\dot{\alpha}_i = -S_i/\tau_i$ .

Based on the definition aforementioned, a dynamic surface position tracking controller can be given by:

$$\begin{cases} \beta_1 = -k_1z_1 + s_2 + \dot{y}_d \\ \beta_2 = -(-\bar{g}_2s_3 + \bar{f}_2 + \hat{\Delta}_2 + \frac{S_1}{\tau_1} + z_1 + k_2z_2)/\bar{g}_2 \\ \alpha_i = -\int_0^t \frac{S_i}{\tau_i} dt, \quad i \in \{1, 2\} \\ S_i = \alpha_i - \beta_i, \quad i \in \{1, 2\} \\ u = -(\bar{f}_3 + \hat{\Delta}_3 + \frac{S_2}{\tau_2} + \bar{g}_2z_2 + k_3z_3)/\bar{g}_3 \end{cases} \quad (13)$$

where  $k_i, i \in \{1, 2, 3\}$  are the adjustable control gains.

Before introducing the stability conclusion, two Young's inequalities are listed in the following as:

$$\begin{aligned} |z_i S_i| &\leq \frac{z_i^2 + S_i^2}{2} \\ |S_i \dot{\beta}_i| &\leq \frac{S_i^2 |\dot{\beta}_i|_{\max}^2}{2\sigma_i} + \frac{\sigma_i}{2} \end{aligned} \quad (14)$$

where  $\sigma_i, i \in \{1, 2\}$  are positive constants.

**Theorem 2.** Consider the EHS (2) together with the dynamic surface position tracking control strategy (13). If the following inequalities

$$\begin{aligned} \frac{1}{2} - k_1 &< 0 \\ \frac{\bar{g}_2}{2} - k_2 &< 0 \\ \frac{1}{2} + \frac{|\dot{\beta}_1|_{\max}^2}{2\sigma_1} - \frac{1}{\tau_1} &< 0 \\ \frac{\bar{g}_2}{2} + \frac{|\dot{\beta}_2|_{\max}^2}{2\sigma_2} - \frac{1}{\tau_2} &< 0 \end{aligned} \quad (15)$$

holds, then, the error functions (10) will converge to zero, which means that the position tracking control purpose of EHS is realized.

**Proof.** In this section, we select the candidate Lyapunov function as:

$$V = \sum_{i=1}^3 z_i^2/2 + \sum_{i=1}^2 S_i^2/2 \quad (16)$$

and divide this Lyapunov function into three cascade parts as:

$$\begin{cases} V_1 = z_1^2/2 + S_1^2/2 \\ V_2 = V_1 + z_2^2/2 + S_2^2/2 \\ V_3 = V_2 + z_3^2/2. \end{cases} \quad (17)$$

As the first step, we take the derivative of  $V_1$  as:

$$\begin{aligned} \dot{V}_1 &= z_1 \dot{z}_1 + S_1 \dot{S}_1 \\ &= z_1(x_2 - \dot{y}_d) + S_1\left(-\frac{S_1}{\tau_1} - \dot{\beta}_1\right) \\ &= z_1(z_2 + \alpha_1 - s_2 - \dot{y}_d) - \frac{S_1^2}{\tau_1} - S_1 \dot{\beta}_1 \\ &= z_1(z_2 + \beta_1 + S_1 - s_2 - \dot{y}_d) - \frac{S_1^2}{\tau_1} - S_1 \dot{\beta}_1. \end{aligned} \quad (18)$$

Substituting  $\beta_1$  in (13) into (18) yields

$$\begin{aligned} \dot{V}_1 &= -k_1 z_1^2 + z_1 z_2 + z_1 S_1 - \frac{S_1^2}{\tau_1} - S_1 \dot{\beta}_1 \\ &\leq -k_1 z_1^2 + z_1 z_2 + z_1 S_1 - \frac{S_1^2}{\tau_1} + |S_1 \dot{\beta}_1| \end{aligned} \quad (19)$$

Combining (14) into (19), it holds that

$$\dot{V}_1 \leq z_1 z_2 + \omega_1 + \frac{\sigma_1}{2} \quad (20)$$

where  $\omega_1 = (\frac{1}{2} - k_1)z_1^2 + (\frac{1}{2} + \frac{|\dot{\beta}_1|_{\max}^2}{2\sigma_1} - \frac{1}{\tau_1})S_1^2$ .

As the second step, we take the derivative of  $V_2$  as:

$$\begin{aligned} \dot{V}_2 &\leq z_1 z_2 + \omega_1 + \frac{\sigma_1}{2} + z_2 \dot{z}_2 + S_2 \dot{S}_2 \\ &\leq z_1 z_2 + \omega_1 + \frac{\sigma_1}{2} + z_2(\bar{f}_2 + \bar{g}_2 x_3 + \Delta_2 - \dot{\alpha}_1 + \dot{s}_2) \\ &\quad + S_2(-\frac{S_2}{\tau_2} - \dot{\beta}_2) \\ &\leq z_1 z_2 + \omega_1 + \frac{\sigma_1}{2} - \frac{S_2^2}{\tau_2} - S_2 \dot{\beta}_2 \\ &\quad + z_2(\bar{f}_2 + \bar{g}_2(z_3 + \beta_2 + S_2 - s_3) + \Delta_2 + \frac{S_1}{\tau_1} + \dot{s}_2) \end{aligned} \quad (21)$$

Substituting  $\beta_2$  in (13) into (21) yields

$$\begin{aligned} \dot{V}_2 &\leq \omega_1 + \frac{\sigma_1}{2} - \frac{S_2^2}{\tau_2} - S_2 \dot{\beta}_2 + z_2 \bar{g}_2 z_3 + z_2 \bar{g}_2 S_2 - k_2 z_2^2 \\ &\leq \omega_1 + \frac{\sigma_1}{2} - \frac{S_2^2}{\tau_2} + |S_2 \dot{\beta}_2| + z_2 \bar{g}_2 z_3 + z_2 \bar{g}_2 S_2 - k_2 z_2^2 \end{aligned} \quad (22)$$

Combining (14) into (22), it follows that

$$\dot{V}_2 \leq z_2 \bar{g}_2 z_3 + \omega_1 + \omega_2 + \frac{\sigma_1}{2} + \frac{\sigma_2}{2} \quad (23)$$

where  $\omega_2 = (\frac{\bar{g}_2}{2} - k_2)z_2^2 + (\frac{\bar{g}_2}{2} + \frac{|\dot{\beta}_2|_{\max}^2}{2\sigma_2} - \frac{1}{\tau_2})S_2^2$ .

As the third step, we take the derivative of  $V_3$  as:

$$\begin{aligned} \dot{V}_3 &\leq \dot{V}_2 + z_3 \dot{z}_3 \\ &\leq z_2 \bar{g}_2 z_3 + \omega_1 + \omega_2 + \frac{\sigma_1 + \sigma_2}{2} \\ &\quad + z_3(f_3 + g_3 u + \Delta_3 + \frac{S_2}{\tau_2} + \dot{s}_3) \\ &\leq \omega_1 + \omega_2 + \frac{\sigma_1 + \sigma_2}{2} - k_3 z_3^2 \end{aligned} \quad (24)$$

We define  $\bar{k} = \max\{|\frac{1}{2} - k_1|, |\frac{\bar{g}_2}{2} - k_2|, |k_3|, |\frac{1}{2} + \frac{|\dot{\beta}_1|_{\max}^2}{2\sigma_1} - \frac{1}{\tau_1}|, |\frac{\bar{g}_2}{2} + \frac{|\dot{\beta}_2|_{\max}^2}{2\sigma_2} - \frac{1}{\tau_2}|\}$ ,  $\sigma = \frac{\sigma_1 + \sigma_2}{2}$ ; then, it can be obtained from (24) that

$$\dot{V}_3 = \dot{V} \leq -\bar{k}V + \sigma,$$

which also illustrates that

$$\dot{V} e^{\int_0^t \bar{k} dt} \leq -\bar{k} V e^{\int_0^t \bar{k} dt} + \sigma e^{\int_0^t \bar{k} dt}. \quad (25)$$

Based on (25), we have

$$\dot{V} e^{\int_0^t \bar{k} dt} + \bar{k} V e^{\int_0^t \bar{k} dt} \leq \sigma e^{\int_0^t \bar{k} dt}$$

and

$$(Ve^{\int_0^t \bar{k} dt})' \leq \sigma e^{\int_0^t \bar{k} dt}. \quad (26)$$

Integrating (26) over the time interval  $(0, t)$ , it follows that

$$\int_0^t (Ve^{\int_0^t \bar{k} dt})' dt \leq \int_0^t \sigma e^{\int_0^t \bar{k} dt} dt, \quad (27)$$

which means

$$V(t)e^{\bar{k}t} - V(0) \leq \frac{\sigma}{\bar{k}} e^{\bar{k}t} - \frac{\sigma}{\bar{k}} \quad (28)$$

and

$$V(t) \leq V(0)e^{-\bar{k}t} + \frac{\sigma}{\bar{k}}(1 - e^{-\bar{k}t}). \quad (29)$$

Here, (29) demonstrates that the error functions (10) realized the uniformly ultimately bounded stability, which also means that the considered EHS (2) realized the position tracking control purpose.  $\square$

The control diagram of the EHS is shown as Figure 2.

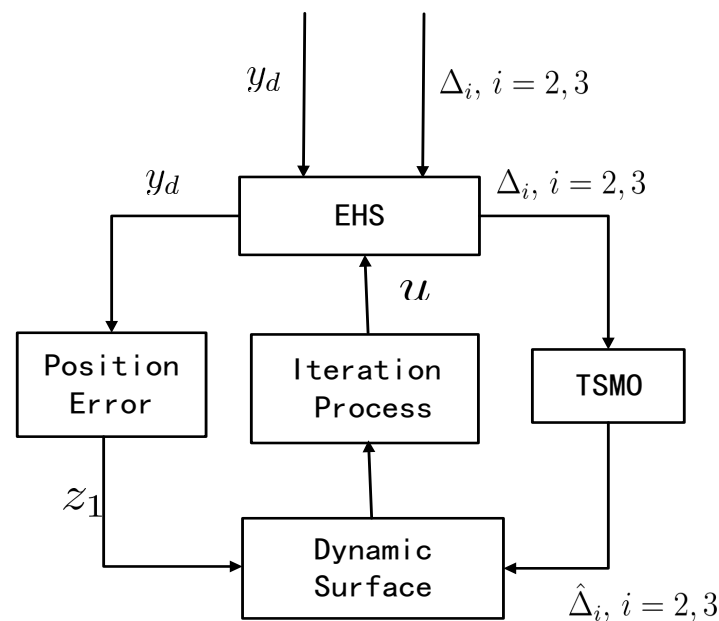


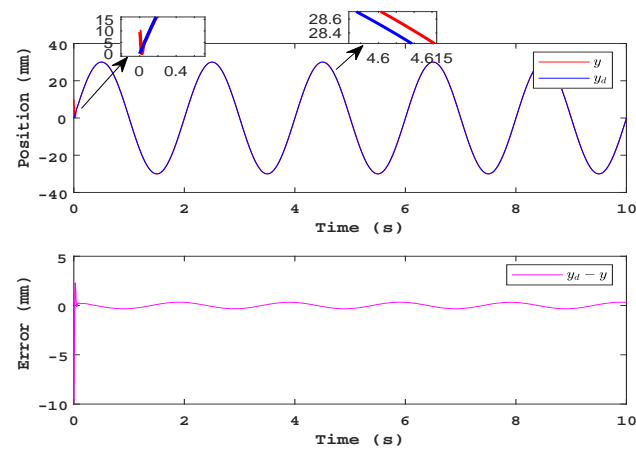
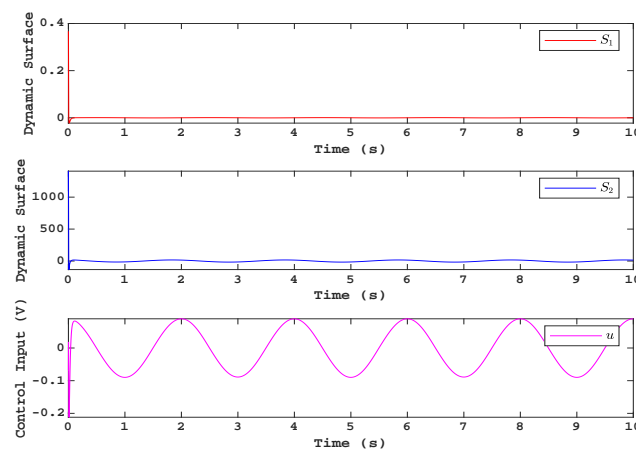
**Figure 2.** The control diagram of EHS.

## 5. Simulation Results

In this section, a virtual EHS model was constructed using the simulink tools in matlab software. The corresponding calculation model is shown in Figure A1 of Appendix A section, and the specific modeling and control parameters are shown in Table 1. Based on this virtual EHS model, the proposed theoretical conclusions can be verified. The specific results are shown in Figures 3–7. Figure 3 provides the tracking trajectory and tracking error of EHS. Figure 4 shows the dynamic surfaces and the control input of the proposed control strategy. Figure 5 provides the estimated values of VSDO and Figure 6 shows the corresponding estimated errors. The dummy control variables of VSDO are provided in Figure 7.

**Table 1.** The simulation parameters of EHS.

| Parameter                | Value                             | Parameter                | Value  |
|--------------------------|-----------------------------------|--------------------------|--|
| $\bar{K}$                | 1000 N/m                          | $\bar{C}_{tl}$           | $2.5 \times 10^{-11} \text{ m}^3/(\text{sPa})$ |
| $\bar{b}$                | 1000 Ns/m                         | $\bar{C}_d$              | 0.62   |
| $\bar{\rho}_e$           | 7000 bar                          | $\bar{\rho}$             | 850 kg/m <sup>3</sup>                          |
| $m$                      | 2 kg                              | $A_p$                    | 2.01 cm <sup>2</sup>                           |
| $V_t$                    | $1.74 \times 10^{-5} \text{ m}^3$ | $\bar{w}$                | 0.024  |
| $p_s$                    | 40 bar                            | $p_r$                    | 1 bar  |
| $K_{sv}$                 | $7.9 \times 10^{-4} \text{ m/V}$  | $ \Delta \rho _{\max}$   | $0.2 \bar{\rho}$                               |
| $ \Delta K _{\max}$      | $0.02 \bar{K}$                    | $ \Delta b _{\max}$      | $0.1 \bar{b}$                                  |
| $ \Delta C_{tl} _{\max}$ | $0.05 \bar{C}_{tl}$               | $ \Delta C_d _{\max}$    | $0.2 \bar{C}_d$                                |
| $ \Delta w _{\max}$      | $0.1 \bar{w}$                     | $ \Delta \rho_e _{\max}$ | $0.05 \bar{\rho}_e$                            |
| $k_{d2}$                 | 2000                              | $k_{d3}$                 | 2500   |
| $D_2$                    | 0.1                               | $D_3$                    | 0.1  |
| $\tau_1$                 | 0.002                             | $\tau_2$                 | 0.002  |
| $k_1$                    | 880                               | $k_2$                    | 780  |
| $k_3$                    | 660                               | $y_d$                    | $30 \sin(\pi t) \text{ mm}$                    |

**Figure 3.** Tracking trajectory and tracking error of EHS.**Figure 4.** Dynamic surfaces and control input of the proposed control strategy.

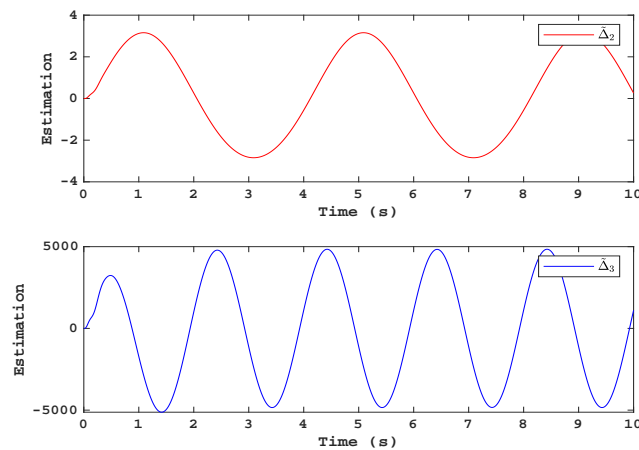


Figure 5. The estimated values of VSDO.

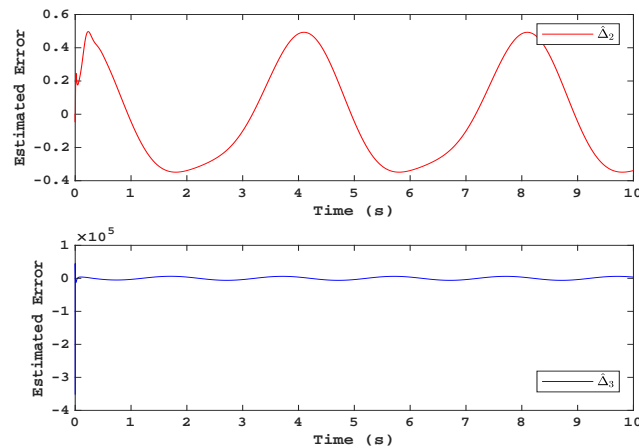


Figure 6. The estimated errors of VSDO.

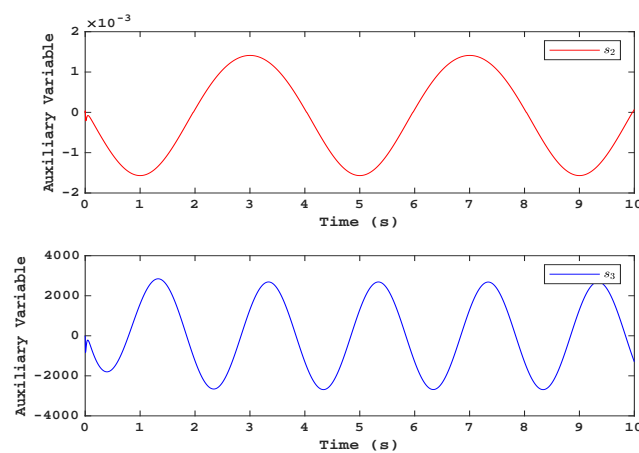
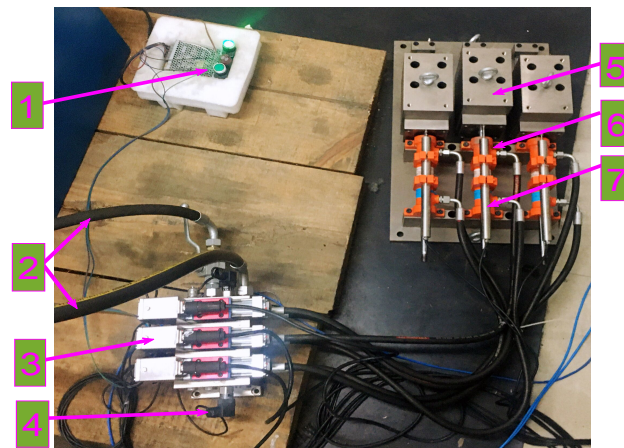


Figure 7. The dummy control variables of VSDO.

## 6. Experiment Results

As Figure 8 shows, the experimental bench consisted of a pump station (Brand: HY-36CC-01/11kw), three nozzle flapper servo valves (Brand: D633-R04K01M0NSM2), and three hydraulic cylinders (Brand: UG1511R25/16-100). The cylinders were activated when the servo valves worked. In this experiment, just one cylinder was activated during the experimental process. The position of the cylinder was collected by the displacement transducer (Brand: JHQ-GA-50), the measuring range was 0–100 mm, and the degree of linearity was  $\pm 0.05\%$ . The pressure between the servo valve was collected by (Brand: BD-sensors-DMP-331).



**Figure 8.** The experimental platform of EHS: 1—Pressure switch, 2—Power supply, 3—Servo valve, 4—Pressure transducer, 5—Mass, 6—Cylinders, and 7—Position transducer.

The nominal values of the EHS parameters are shown in Table 1, and the desired trajectory was given as  $y_d = 20 \sin(\pi t)$  mm. Then, the control parameters were selected as  $k_{d2} = 1333$ ,  $k_{d3} = 1666$ ,  $D_2 = 3$ ,  $D_3 = 2$ ,  $\tau_1 = \tau_2 = 0.002$ ,  $k_1 = 660$ ,  $k_2 = 500$ , and  $k_3 = 220$ . Then, the experimental results are shown in Figures 9–13. Figure 9 shows the tracking trajectory and tracking error of EHS under the desired trajectory  $y_d = 20 \sin(\pi t)$  mm. The dynamic surface values  $S_i$ ,  $i \in \{1, 2\}$  and control input  $u$  are provided in Figure 10. The estimation values and estimated errors of VSDO are exhibited in Figures 11 and 12. Finally, the dummy variables  $s_i$ ,  $i \in \{2, 3\}$  are shown in Figure 13.

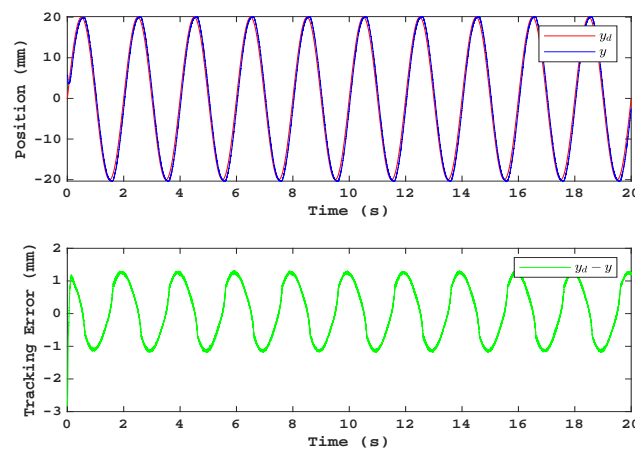


**Figure 9.** Tracking trajectory and tracking error of the EHS in the experiment.

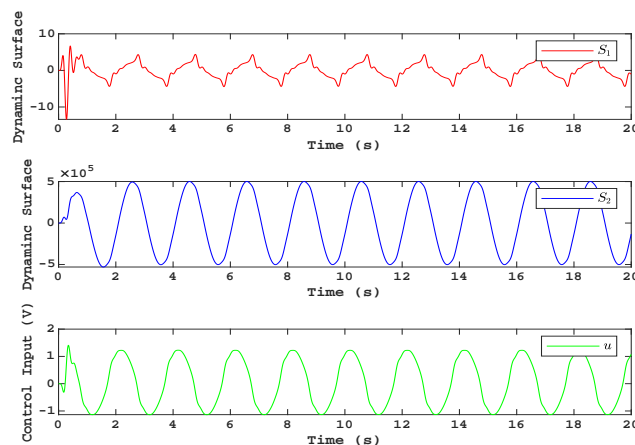


**Figure 10.** Dynamic surfaces and control input of the proposed control strategy in the experiment.

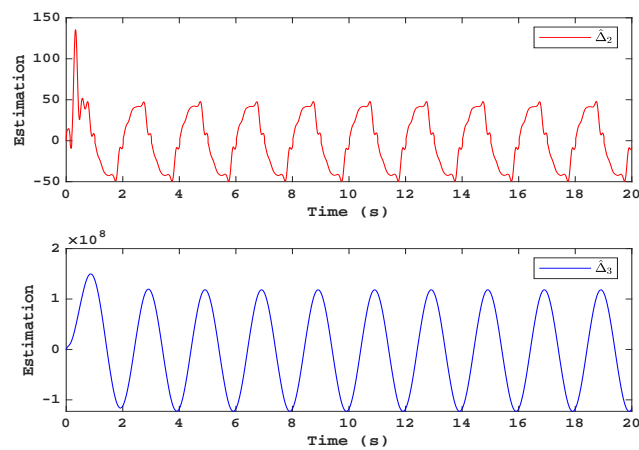


Figure 11. The estimated values of the VSDO in the experiment.

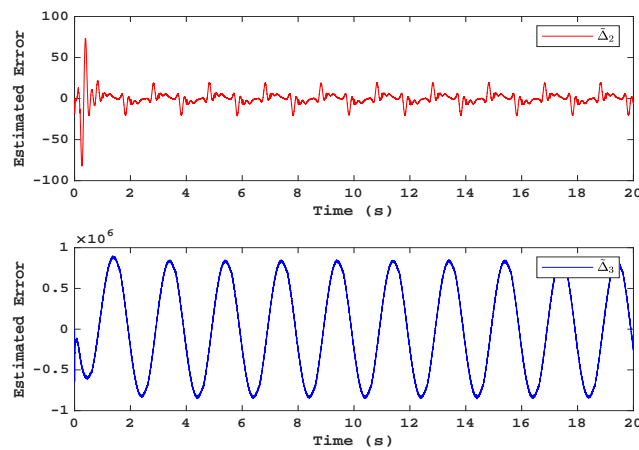


Figure 12. The estimated errors of the VSDO in the experiment.

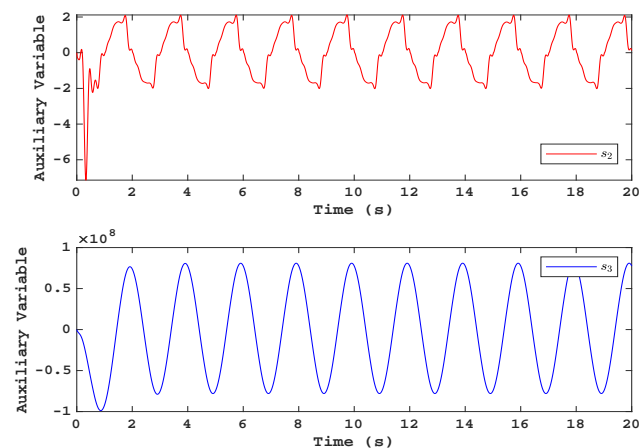


Figure 13. The dummy control variables of the VSDO in the experiment.

## 7. Discussion

This paper provides a position tracking control strategy for an EHS. Firstly, terminal sliding mode observer (TSMO) was introduced to estimate the parametric uncertainty of the EHS. The existing disturbance estimation strategies, such as high gain observer, adaptive observer, and extended state observer are only focused on estimated accuracy. However, TSMO focuses not only on the estimated accuracy but also on the estimated velocity. Secondly, based on the proposed TSMO, a dynamic surface controller was designed for the EHS to realize the position tracking control purpose. Different from the conventional



backstepping controller for EHS, a dynamic surface controller can effectively overcome the differential explosion during the iterative process. Although the theoretical results of this paper are superior to the related works before, a shortcoming should be pointed out, in that the difficulty of adjusting the controller parameters is increasing.

## 8. Conclusions

In this paper, a kind of variable structure disturbance observer was presented to estimate the parametric uncertainty of an EHS. Based on the presented VSDO strategy, a dynamic surface position tracking controller was also presented. Different from the existing conventional results on the tracking control of EHS, the controller provided in this paper was constructed via a dynamic surface control strategy to overcome the differential explosion. The effectiveness of proposed control method was verified by simulations and experiments. In the future, more control characteristics, such as input delay or robustness, will be investigated.

**Author Contributions:** S.L. took charge of the writing of this article; Q.G. and Y.Y. conceived and designed the architecture of this paper; K.Z. and L.C. performed the simulations and experiments. All authors have read and agreed to the published version of the manuscript.

**Funding:** This research was funded by National Natural Science Foundation of China (Grant Nos. 52175046, 51775089, 51975024, 12072068 and 11872147) and the Sichuan Science and Technology Program (Grant Nos. 22CXRC0089 and 22ZDYF3178).

**Institutional Review Board Statement:** This study is not applicable for involving humans or animals.

**Informed Consent Statement:** Not applicable.

**Data Availability Statement:** Not applicable.

**Acknowledgments:** This work was supported by the National Natural Science Foundation of China (Grant Nos. 52175046, 51775089, 51975024, 12072068 and 11872147) and the Sichuan Science and Technology Program (Grant Nos. 22CXRC0089 and 22ZDYF3178).

**Conflicts of Interest:** The authors declare no conflict of interest.

## Nomenclature

|              |  |
|--------------|--|
| $K_{sv}$     | Gain voltage of the servo valve              |
| $u$          | Control voltage of the servo valve           |
| $C_d$        | Discharge coefficient                        |
| $w$          | Area gradient of the servo valve             |
| $p_s$        | Supply pressure                              |
| $p_r$        | Return pressure                              |
| $p_L$        | Load pressure of cylinder                    |
| $y, \dot{y}$ | The cylinder position and velocity           |
| $\rho$       | Density of hydraulic oil                     |
| $C_{tl}$     | Coefficient of the leakage of the cylinder   |
| $\beta_e$    | Effective bulk modulus                       |
| $A_p$        | Annulus area of the cylinder chamber         |
| $V_t$        | Volume of the hydraulic power mechanism      |
| $m$          | Load mass coefficient                        |
| $b$          | Viscous damping coefficient                  |
| $K$          | Spring stiffness coefficient of the cylinder |

## Appendix A

In this section, the calculation model of EHS from Matlab Simulink has been provided in Figure A1.

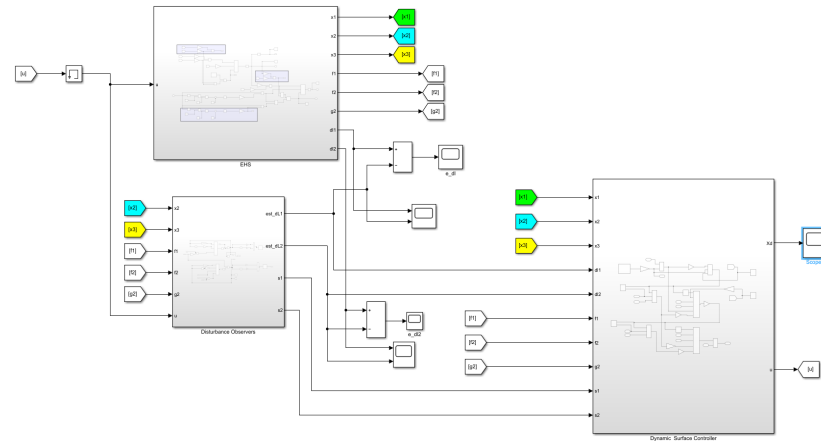


Figure A1. The calculation model of EHS from Matlab.

## References

- Li, D.; Shang, M.; Ma, G. An electro-hydraulic system on anti-sticking for the drilling rig underground coal mine. In Proceedings of the 2019 IEEE 8th International Conference on Fluid Power and Mechatronics (FPM), Wuhan, China, 10–13 April 2019; pp. 951–956.
- Zhang, H.; Han, W.; Xiong, L.; Xu, S. Design and research on hydraulic control unit for a novel integrated-electro-hydraulic braking system. In Proceedings of the 2016 IEEE Transportation Electrification Conference and Expo, Asia-Pacific (ITEC Asia-Pacific), Busan, Korea, 1–4 June 2016; pp. 139–144.
- Kuai, T.; Zou, Q.; Zhao, X.; Zhao, C.; Ren, J.; Le, G. Electro-hydraulic control techniques and applications of launching systems. In Proceedings of the 2019 4th International Conference on Electromechanical Control Technology and Transportation (ICECTT), Guilin, China, 26–28 April 2019; pp. 49–52.
- Fales, R.; Kelkar, A. Robust control design for a wheel loader using  $H_\infty$  and feedback linearization based methods. *ISA Trans.* **2009**, *48*, 313–320. [[CrossRef](#)] [[PubMed](#)]
- Yang, Y.; Ma, L.; Huang, D. Development and repetitive learning control of lower limb exoskeleton driven by electro-hydraulic actuators. *IEEE Trans. Ind. Electron.* **2017**, *64*, 4169–4178. [[CrossRef](#)]
- Zhao, J.; Wang, J.; Wang, S. Fractional order control to the electrohydraulic system in insulator fatigue test device. *Mechatronics* **2013**, *23*, 828–839. [[CrossRef](#)]
- Won, D.; Kim, W.; Shin, D.; Chung, C.C. High-gain disturbance observer-based backstepping control with output tracking error constraint for electro-hydraulic systems. *IEEE Trans. Control Syst. Technol.* **2015**, *23*, 787–795. [[CrossRef](#)]
- Guo, Q.; Zhang, Y.; Celler, B.G.; Su, S.W. Neural adaptive backstepping control of a robotic manipulator with prescribed performance constraint. *IEEE Trans. Neural Netw. Learn. Syst.* **2019**, *30*, 3572–3583. [[CrossRef](#)] [[PubMed](#)]
- Cheng, L.; Zhu, Z.C.; Shen, G.; Wang, S.; Li, X.; Tang, Y. Real-time force tracking control of an electro-hydraulic system using a novel robust adaptive sliding mode controller. *IEEE Access* **2020**, *8*, 13315–13328. [[CrossRef](#)]
- Ren, H.P.; Jiao, S.S.; Wang, X.; Kaynak, O. Fractional order integral sliding mode controller based on neural network: Theory and electro-hydraulic benchmark test. *IEEE/ASME Trans. Mechatron.* **2021**. [[CrossRef](#)]
- Ma, W.; Deng, W.; Yao, J. Continuous integral robust control of electro-hydraulic systems with modeling uncertainties. *IEEE Access* **2018**, *6*, 46146–46156. [[CrossRef](#)]
- Yang, G.; Yao, J.; Le, G.; Ma, D. Adaptive integral robust control of hydraulic systems with asymptotic tracking. *Mechatronics* **2016**, *40*, 78–86. [[CrossRef](#)]
- Guo, Q.; Chen, Z.L. Neural adaptive control of single-rod electrohydraulic system with lumped uncertainty. *Mech. Syst. Signal Process.* **2021**, *146*, 106869. [[CrossRef](#)]
- Yao, Z.; Yao, J.; Yao, F.; Xu, Q.; Xu, M.; Deng, W. Model reference adaptive tracking control for hydraulic servo systems with nonlinear neural-networks. *ISA Trans.* **2020**, *100*, 396–404. [[CrossRef](#)] [[PubMed](#)]
- Wang, S.; Xu, Q.; Lin, R.; Yang, M.; Zheng, W.; Wang, Z. Feedback linearization control for electro-hydraulic servo system based on nonlinear disturbance observer. In Proceedings of the 2017 36th Chinese Control Conference (CCC), Dalian, China, 26–28 July 2017; pp. 4940–4945.
- Chen, G.; Jia, P.; Yan, G.; Liu, H.; Chen, W.; Jia, C.; Ai, C. Research on Feedback-Linearized Sliding Mode Control of Direct-Drive Volume Control Electro-Hydraulic Servo System. *Processes* **2021**, *9*, 1676. [[CrossRef](#)]

17. Ma, Z.; Ma, H. Adaptive fuzzy backstepping dynamic surface control of strict-feedback fractional-order uncertain nonlinear systems. *IEEE Trans. Fuzzy Syst.* **2019**, *28*, 122–133. [[CrossRef](#)]
18. Niu, B.; Li, H.; Zhang, Z.; Li, J.; Hayat, T.; Alsaadi, F.E. Adaptive neural-network-based dynamic surface control for stochastic interconnected nonlinear nonstrict-feedback systems with dead zone. *IEEE Trans. Syst. Man Cybern. Syst.* **2018**, *49*, 1386–1398. [[CrossRef](#)]
19. Shi, X.; Cheng, Y.; Yin, C.; Huang, X.; Zhong, S.M. Design of adaptive backstepping dynamic surface control method with rbf neural network for uncertain nonlinear system. *Neurocomputing* **2019**, *330*, 490–503. [[CrossRef](#)]
20. Jing, C.; Xu, H.; Jiang, J. Dynamic surface disturbance rejection control for electro-hydraulic load simulator. *Mech. Syst. Signal Process.* **2019**, *134*, 106293. [[CrossRef](#)]
21. Liu, Y.; Fang, J.; Tan, K.; Huang, B.; He, W. Sliding Mode Observer with Adaptive Parameter Estimation for Sensorless Control of IPMSM. *Energies* **2020**, *13*, 5991. [[CrossRef](#)]
22. Bao, D.; Wu, H.; Wang, R.; Zhao, F.; Pan, X. Full-Order Sliding Mode Observer Based on Synchronous Frequency Tracking Filter for High-Speed Interior PMSM Sensorless Drives. *Energies* **2020**, *13*, 6511. [[CrossRef](#)]
23. Zhao, Y.; Yu, H.; Wang, S. An Improved Super-Twisting High-Order Sliding Mode Observer for Sensorless Control of Permanent Magnet Synchronous Motor. *Energies* **2021**, *14*, 6047. [[CrossRef](#)]
24. Wang, Q.; Wu, Z. Robust output feedback control for input-saturated systems based on a sliding mode observer. *Circuits Syst. Signal Process.* **2021**, *40*, 2267–2281. [[CrossRef](#)]